

WEAK TURBULANT FLUXES ESTIMATION IN SURFACE WATER WAVE SPECTRUM

Igor V. Lavrenov

State Research Center of the Russian Federation

Arctic and Antarctic Research Institute, Bering 38, 199397, St. Petersburg, Russia, e-mail: lavren@aari.nw

1 INTRODUCTION

The traditional method of wind wave estimation is based on the equation of wind wave spectrum energy evolution. For the first time the attitude for wind wave estimation based on the wind wave balance equation was proposed by V. M. Makkaviev (Makkaviev, 1937).

It was one of the first attempts to describe mathematically a wind wave development, which found its practical application. In its simplest form the equation describes evolution of wind wave energy depending on average wind speed and dissipation. The investigation results of the so-called “energetic” direction allowed in 40-s of the last century to develop elementary practical methods of calculations and wind wave forecasting. The new considerable step on the way of theoretical description of natural sea surface development was made after 50-s of the last century when the researches started investigating wind waves from the spectral point of view using the theory of probability functions. Wind waves were considered to be a random process and described on the bases on joint application of hydrodynamic and statistical methods. The Fourier presentation of random wind wave process allowed decomposing it on harmonic components. Their behaviour could be considered from the point of view of the classical wave monochromatic theory. The works published after 1956 (Longuet—Higgins 1957; Longuet—Higgins et al. 1960, 1961, 1962, 1964; Phillips, 1957, 1958; Miles 1957, 1960; Hasselmann, 1960, 1962, 1963, etc.) founded the principles of modern physical notion of wind wave development.

Nowadays, the wave energy balance equation is written in the form of the kinetic equation describing evolution of spectral density of wave action under the influence of external fields which are wind speed, currents, shallow waters, ice cover, etc. (Lavrenov, 2003). Its generalized form the equation can be presented as :

$$\frac{dN}{dt} = \frac{\partial N}{\partial t} + \frac{\partial}{\partial \vec{r}}(N\vec{r}) + \frac{\partial}{\partial \vec{k}}(N\vec{k}) + \frac{\partial}{\partial \omega}(N\dot{\omega}) = G \quad (1)$$

where N is wave action density; \vec{r}, \vec{k} are spatial and wave vectors, ω is wave absolute frequency, G is source function, describing different physical mechanisms forming wind wave spectrum.

A study of these physical mechanisms is one of the central problems associated with wave numerical simulations (Davidan et al., 1985; Ocean wave modeling, 1985; Komen et al., 1994; Massel, 1996; Young, 1999; Lavrenov, 2003, etc).

It is assumed that the source function G in deep water includes at least three main components: G_{in} – wind wave energy input, G_{ds} – wave energy dissipation and G_{nl} – non-linear energy transfer within the wave spectrum.

The component of the wind wave energy input G_{in} is usually determined with the help of the relation based on the model of averaged airflow interaction with wave (Miles, 1960). Although it was proposed in 1957, this model is still used nowadays. The mechanism specified by using full-scale observation data (Snyder et al., 1981) can be described as follows:

$$G_{in}(\omega, \beta) = \max \left\{ 0; 0.25 a_1 \frac{\rho_a}{\rho_w} \omega \times \left(a_2 \frac{U_{10}}{c} \cos(\beta - \beta_U) - 1 \right) S(\omega, \beta) \right\}, \quad (2)$$

where: U_{10} is the wind speed at 10 m level; $\beta - \beta_U$ is the angle between the wind speed and the direction of wave spectral component propagation; a_1 and a_2 are the parameters with the value of about 1.0. As it follows from (2), the wind energy is supplied to the wave spectrum range at $a_2(U_{10}/c) \cos(\beta - \beta_U) > 1$.

Lately, the relation (2) is also expressed with the help of the dynamic velocity (or friction velocity) U_* instead of wind speed U_{10} . The most accurate numerical modeling of the statistical structure of atmospheric boundary layer above sea surface based on the numerical solution of the Reynold two-dimensional equations is described in papers (Chalikhov, 1986; Burgers&Makin, 1992,

Chalikov&Belevich, 1995; Belevich&Neelov, 1999; Makin&Kudriavtsev, 2002; Kudriavtsev& Makin, 2004). It is shown that the wind wave energy input term G_{in} can be expressed as:

$$G_{in}(\omega, \beta) = B_U \omega S(\omega, \beta) \quad (3)$$

where B_U is a non-dimensional parameter of wind-wave interaction.

The parameter B_U is thoroughly studied in (Chalikov&Belevich, 1995; Makin&Kudriavtsev, 2002; Kudriavtsev&Makin, 2004). There are three main differences of this parameterization from the Snyder's empirical relation. First, a value of the function becomes negative for waves propagating faster than the wind speed. In this case the wave phase speed projection onto the wind direction is compared with the wind speed. If the dynamic wind pressure on the frontal wave surface is higher in comparison with the rear surface pressure, it causes the appearance of the energy flow directed from waves to wind. Second, the integral energy flow to waves becomes 2-3-fold less in case of fully developed wind sea. It is determined by the energy outflux from low-frequency components propagating faster than the wind speed and a relatively small influx to the waves with velocity close to wind speed. Third, in the high frequency range, a greater energy flux compared to the Snyder's formula (2), is estimated with the help of the approximation (3) since B_U is proportional to ω^2 at large frequency value ω . The difference in the integral value of this wind wave energy input and the Snyder's ratio becomes smaller for the initial stage of wind sea development. It should be noted that the value of the wind wave energy input function used in the WAM model (Komen et al., 1994) is also smaller in comparison with the Snyder's value. As there is not only an energy flux from wind to waves, but also a flux from waves to wind in the wave/wind interaction mechanism (3), it becomes possible to use this mechanism for achieving more rapid spectrum shape stabilization on the developed wave stage. The parameter approximation B_U is compared with the observation data. Their consistency within the confidence interval of the measurement results is shown in papers (Chalikov&Belevich, 1995; Makin&Kudriavtsev, 2002; Kudriavtsev&Makin, 2004).

The mechanism of wave energy dissipation still remains the least studied. The absence of its definite physical basis is, probably, connected with difficulties in the theoretical description of wind sea dissipation within the frames of the existing

concepts of hydrodynamics. The mechanism of wave dissipation in deep water is supposed to be mainly associated with wave crest breaking (whitecapping). However, there is no scientifically recognised opinion whether its adequate dependence on energy spectral density is linear or non-linear.

There are some empirical approximations for wave dissipation in wind wave modelling (Abuzyarov, 1981; Davidan et al., 1985; Ocean wave modelling, 1985). A generalised review concerning this problem is put forward in (Komen et al., 1994; Banner et al., 2001). K.Hasselmann (1974) proposed the wave energy dissipation parameterisation, connected with wave breaking. In his opinion it can be considered as random distribution of perturbing forces, making up pressure pulsations with small scales in space and time in comparison with the proper wave length and period. All the weak processes are shown to be locally non-linear on the average, producing a source function, which is quasilinear relatively to interactions of the lowest order. In this case the source function dissipation is presented in the form of linear dependence on the spectrum. It is multiplied by the value depending integrally on the whole spectrum. The wave dissipation used in the WAM model (The WAM model, 1988; Komen et al., 1994) connected with wave breaking is accepted in the form of the quasi-linear approximation, as it is suggested by G.Komen (1984) on the basis of the Hasselmann model:

$$G_{ds}(\omega, \beta) = -c_{ds1} \bar{\omega} \left(\frac{\omega}{\bar{\omega}} \right) \left(\frac{\bar{\alpha}}{\alpha_{PM}} \right)^m S(\omega, \beta) \quad (4)$$

where c_{ds1} , c , n and m are the model parameters; $\bar{\omega}$ is the mean frequency of the wave spectrum; α_{PM} is the constant of the Pierson-Moskovits spectrum; $\bar{\alpha} = m_0 \bar{\omega}^4 / g^2$,

$c_{ds1} = 3.33 \cdot 10^{-5}$, $n = 2$, $m = 2$. The dissipation function (4) depends linearly on the spectrum as well as on its integral parameters. A peculiarity of the dissipation parameterization is in permitting (totally with other items of the source function) to obtain spectra of fully developed sea in the form of the Pierson-Moskovits approximations. Due to initial concept of wave breaking considered as random distribution of disturbing forces with small scales, the use of the relation (4) is limited in high-frequency spectral area. As a consequence, the relation (4) does not guarantee the stable convergence of wave energy balance equation solution to value of equilibrium interval spectrum in the area of the high frequencies. It happens due to wind energy input and dissipation being linear on

the spectrum intensity. That is why an unjustified small time step and additional limitations on spectral value and source function are used in numerical simulation of the WAM model (The WAM model, 1988; Komen et. al., 1994).

There are some other dissipation parameterizations, depending non-linearly on the spectral density function. For the first time they were investigated more than 40 years ago in the first semi-empirical wind wave models (Abuzyarov, 1981; Davidan et al., 1985; Ocean wave modelling, 1985). O.Phillips (1985) suggested a theoretical basis for wave energy dissipation depending non-linearly on spectral density. In contrast to K.Hasselmann, he put forward the idea that wave breaking was of local character, i.e. energy losses due to dissipation of concrete spectral component depended on its spectral density of energy not determined by the integral parameters of the whole spectrum. He came to the conclusion that wind wave energy input, dissipation and non-linear interaction were of the same order in the spectrum equilibrium range. Using the wave energy balance he found out that the dissipation should depend cubically on the spectrum:

$$G_{ds} = -c_2 \omega k^8 S^3(\omega, \beta) \quad (5)$$

where C_{ds} is a constant.

It should be noted that wave energy dissipation in the form (5) produces more stable numerical convergence limiting spectrum value at large frequencies. However, it seems to be rather doubtful to use the expression (5) for low frequency range of wind waves and swell simulations.

Polnikov (1991; 1994; 1995) proposed alternative model of wind wave dissipation based on wave interaction with turbulence generated by wave breaking. The dissipation term is found to be proportional to second order of spectrum density. Davidan (1985) analyzing theoretical and experimental results came to the conclusion that there was a difference of the dissipative mechanisms in various frequency spectrum ranges. At least, one thing could be set for sure that in a low frequency spectral band with practically no wind wave energy, the dissipative value was so small that it could be neglected. At the same time the dissipation was sharply increased in a high frequency band where the wind energy input was important. In other words, the dissipation could be dependent on wind speed as well.

It should be noted that Tolman and Chalikov (1996) came to the same conclusions as Davidan. They

investigated source function in the wind wave models of the third generation and found out principal difference of physical mechanism effect in various bands of frequency spectrum. The whole frequency range is divided into three sections: low, transitional and high-frequency parts, the dissipative mechanism being determined separately for every section with different dependences on wave spectrum density.

One of the most important mechanisms in wind wave spectrum formation is non-linear energy transfer, based on the kinetic equation (Hasselmann, 1962,1963; Zakharov, 1968). In terms of wave action spectrum the non-linear energy transfer function is as follows:

$$G_{nl} = \iiint T(\vec{k}, \vec{k}_1, \vec{k}_2, \vec{k}_3) \delta(\vec{k} + \vec{k}_1 - \vec{k}_2 - \vec{k}_3) \times \\ \times \delta(\omega + \omega_1 - \omega_2 - \omega_3) \times \\ \times \{N_2 N_3 (N + N_1) - N_1 N (N_2 + N_3)\} d\vec{k}_1 d\vec{k}_2 d\vec{k}_3 \quad (6)$$

where $N_i = N(\vec{k}_i)$ is the spectral density of wave action; $T(\vec{k}, \vec{k}_1, \vec{k}_2, \vec{k}_3)$ is the core function of non-linear interaction between waves; $\delta(\vec{k})$ and $\delta(\omega)$ are delta-function describing the resonance interaction between four wave components:

$$\vec{k} + \vec{k}_1 = \vec{k}_2 + \vec{k}_3; \quad (7a)$$

$$\omega + \omega_1 = \omega_2 + \omega_3. \quad (7b)$$

One of the most important features of the equation (6) is that the constants of motion such as wave action, energy and momentum, are preserved in spectrum evolution:

$$N = \int N(\vec{k}) d\vec{k} \\ E = \int \omega(\vec{k}) N(\vec{k}) d\vec{k} \\ \vec{K} = \int \vec{k} N(\vec{k}) d\vec{k}. \quad (8)$$

The equation (6) has been a subject of analytical study and numerical modelling for almost four decades (Hasselmann 1962,1963; Hasselmann et al. 1985; Komen et al. 1994; Komatsu and Masuda 1996; Lavrenov 1998, 2001; Polnikov 1993; Resio and Perrie 1991; Webb 1978; etc.).

The main progress in its analytical study is achieved by V.Zakharov with his colleagues (1966,1982). Two physically grounded frequency spectra are determined (Zakharov & Zaslavskii, 1982, 1983a,b) for isotropic case as follows:

$$S_1(\omega) = C_1 \sqrt[3]{Q g^4 / \omega^{11}};$$

$$S_2(\omega) = C_2 \sqrt[3]{P g^4 / \omega^{12}} \quad (9)$$

where Q is a wave action flow; P is a wave energy flow. The first solution is interpreted as a model with energy input located at $\omega = \infty$, and the spectrum being determined by wave action flow directed to the long-wave area $\omega = 0$. The second solution describes the wave energy input at $\omega = 0$, forming an energy flow into the dissipation area $\omega = \infty$. Both solutions are obtained analytically in accordance with rather strict mathematical notions. They are justified within the frames of physical hypotheses accepted by the authors: the weak turbulence approximation in the presence of transparency interval, with the wave energy input and dissipation being not essential.

Further development of this investigation is fulfilled in papers (Pushkarev et al., 2001; Lavrenov et al., 2002). So, in order to study the time establishment of stationary spectra the kinetic equation (6) is investigated numerically taking into account an external generating force and dissipation. Wave energy input is located at high frequency range. Two stages of wave development are revealed: unstable wave energy growth within a range of external force impact and a fast formation of an “energy spectrum tail” in high frequency range with establishment of a steady state, close to the Kolmogorov-Zakharov weak turbulent law: $S \sim \omega^{-4}$.

It should be noted that according to the weak turbulence theory the general Kolmogorov frequency–angular spectrum is defined by following fluxes: wave energy P , wave action Q and momentum M . In a general case (Zakharov et al., 1992) the spectrum is as follows:

$$S(\omega, \beta) = \frac{g^{4/3} P^{1/3}}{\omega^4} F\left(\frac{\omega Q}{P}, \frac{g M}{\omega P}, \cos \beta\right) \quad (10)$$

The function F can be expanded into the Taylor series for the large value ω and the spectrum $S(\omega, \beta)$ can be approximated as follows:

$$S(\omega, \beta) \cong \frac{g^{4/3} P^{1/3}}{\omega^4} \left(\alpha_0 + \alpha_1 \frac{g M \cos(\beta)}{\omega P} + \dots \right) \quad (11)$$

where α_0 and α_1 are the first and the second Kolmogorov constants, which are coefficients of the spectral density expansion into Fourier series.

The reliable estimations of the Kolmogorov constants are found out to be equal to $\alpha_0 = 0.31 \pm 0.03$, $\alpha_1 = 0.24 \pm 0.03$ (Lavrenov et al., 2002).

In spite of these results, a problem of spectrum formation for more general case remains still open. So, the questions appear whether the weak turbulence theory is able to describe wind wave spectrum development in field conditions, whereas the wind energy input and dissipation are localised within a definite frequency range, which does not coincide with different ends of the infinite frequency range $[0, \infty]$, as it was assumed by the theory (Zakharov and Zaslavskii, 1982).

There appear the following questions and the attempts are undertaken to answer them in this paper. What is a ratio between wave energy, action and momentum fluxes directed into high and low frequency ranges? What is the value of wave energy dissipation estimated with the help of weak turbulence theory? Various approximations of wind wave dissipation have been mentioned earlier. Namely, the WAM model type dissipation covering main frequency domain and Zakharov’s type located in the high frequency range. A question appears which type of dissipation is the most reliable from the physical point of view.

Understanding the importance of this problem it is decided to produce detailed numerical simulations of the energy balance equation with different type of source function using the numerical integration method of the highest accuracy (Lavrenov, 1998, 2001). The main attention will be paid to estimation of wave energy, action and momentum fluxes in wind wave spectrum.

2. PROBLEM FORMULATION

Two stages of investigations are considered in the paper. The first one is connected with theoretical consideration of the academic test proposed by V. Zakharov with source function below. The second one considers application of theoretical notions solving the problem connected with utilization of source function for natural wind wave development.

Now the wave action balance equation written in plane surface (deep water and without current case) is considered:

$$\frac{\partial N}{\partial t} + C_{gx} \frac{\partial N}{\partial x} + C_{gy} \frac{\partial N}{\partial y} = G = G_{nl} + F - \gamma N \quad (12)$$

where G_{nl} is the non-linear energy transfer function (6); γ is an attenuation depending on the frequency ω as follows :

$$\gamma = \begin{cases} C_1(\omega_1 - \omega)^2, & \text{for } \omega < \omega_1 \\ 0, & \text{if } \omega_1 < \omega < \omega_4 \\ C_2(\omega - \omega_4)^2, & \text{for } \omega > \omega_{4x} \end{cases} \quad (13),$$

where $C_{1,2}$ are constants.

The value F is an external active force: $F = f N$ with f being not equal to zero within the frequency range: $\omega_2 < \omega < \omega_3$ (where $\omega_1 < \omega_2 < \omega_3 < \omega_4$). It is equal to the following angular function:

$$f = \begin{cases} Q \cos^n(A\beta), & \text{if } \cos(A\beta) > 0 \\ 0, & \cos(A\beta) \leq 0 \end{cases}, \quad (14)$$

where Q is a normalising function, providing the same integral value for various n and A :

$$\int_{-\pi}^{\pi} f(\beta) d\beta = Const, \text{ where } Const \text{ is a constant.}$$

In order to get a representative number of numerical results in grid points the following value ratio between frequencies is used: $\omega_{i+1} \approx 2.0 \omega_i$, where $i = 1, 2, 3, 4$, correspondingly; $\omega_1 = 0.5$ rad/sec

In numerical simulation the spectrum is presented using 70 frequencies and 96 directions. As far as the solution is obtained for a large time scale (up to 10^6 seconds) an optimal numerical algorithm of non-linear energy transfer computation (Lavrenov, 1998; 2001) is used.

3. NUMERICAL RESULTS FOR ACADEMIC CASE

3.1 Spectrum evolution

At the beginning the numerical results for spatial uniform case of the equation (12) are considered, i.e.

$$\frac{\partial N}{\partial t} = G_{nl} + F - \gamma N \quad (15)$$

The first numerical simulation for isotropic source function with $n = 0.0$ and $A = 1.0$ is carried out. Results for frequency spectrum evolution defined as:

$$S(\omega) = \int_{-\pi}^{\pi} S(\omega, \beta) d\beta = \int_{-\pi}^{\pi} N(\omega, \beta) 2\omega^4 / g^2 d\beta \quad (15)$$

are presented in Fig.1.

Frequency spectrum values are presented in the logarithmic scale for the following time steps: $4 \cdot 10^3$, $6 \cdot 10^3$, $8 \cdot 10^3$, 10^4 , $1.2 \cdot 10^4$, $1.4 \cdot 10^4$, $1.6 \cdot 10^4$, $1.8 \cdot 10^4$, $2.0 \cdot 10^4$, $5.0 \cdot 10^4$, 10^5 and $2.0 \cdot 10^5$ sec., respectively.

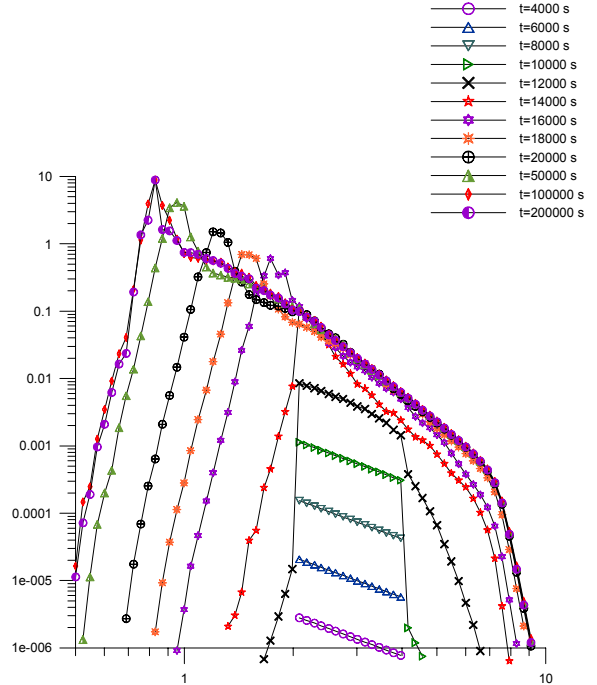


Fig. 1. Spectrum evolution in time for isotropic case

Three different stages can be defined in the wave spectrum evolution. At the first stage a spectrum unstable growth is observed within the range of the external force action: $2.0 < \omega < 4.0$ rad/s. The spectrum is quickly increased at more than 5 orders. The duration of this time interval is estimated as: $t \approx 10^4$ sec.

A high frequency spectrum development is observed at the second stage of spectrum evolution. As it is seen the frequency spectrum is penetrated into the high frequency range ($\omega \geq 4.0$ rad/s), where its value becomes larger, approaching some constant value. This time interval is estimated as $1.0 \cdot 10^4 < t \leq 1.4 \cdot 10^4$ sec. After that the spectrum remains almost constant at high frequency range.

The third stage of spectrum evolution is observed at a larger time period. It is characterized by a slow spectrum evolution into a low frequency range ($\omega < 2.0$ rad/s). The spectrum value becomes larger penetrating into a smaller frequency range with decreasing speed.

Time evolution of spectrum maximum frequency as a function of time is presented in Fig. 2

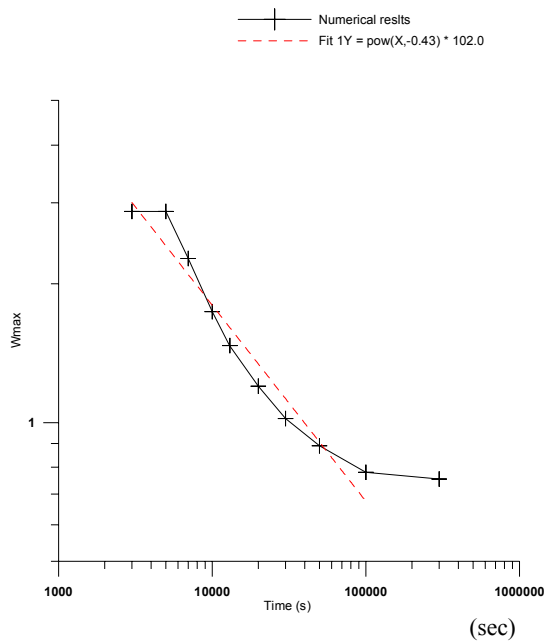


Fig. 2. Evolution of spectrum maximum frequency in time: (+) –numerical simulation results; (-----) – approximations $\omega_p \approx t^{-0.43}$

Frequency of spectrum maximum becomes smaller in time. This dependence can be approximated as $\omega_p \approx t^{-0.43}$. It is similar to the one obtained with the help of field experimental data analysis (Davidan et al., 1985).

Spectrum evolution is stopped at larger time due to influence of low energy dissipation defined in the problem formulation (15). A time interval of spectrum stabilization is estimated as $t \approx 10^5$ sec. After that the low frequency spectrum value remains almost constant (Fig.1).

Total wave energy, wave action and momentum time evolution are presented in Fig.3. As it is seen these values become almost stable after $t \approx 10^5$ sec. It is another evidence of the problem solution approaching its stable state.

Stabilized frequency spectrum is presented in Fig.4. There are two frequency areas, which can be approximated by different power dependencies.

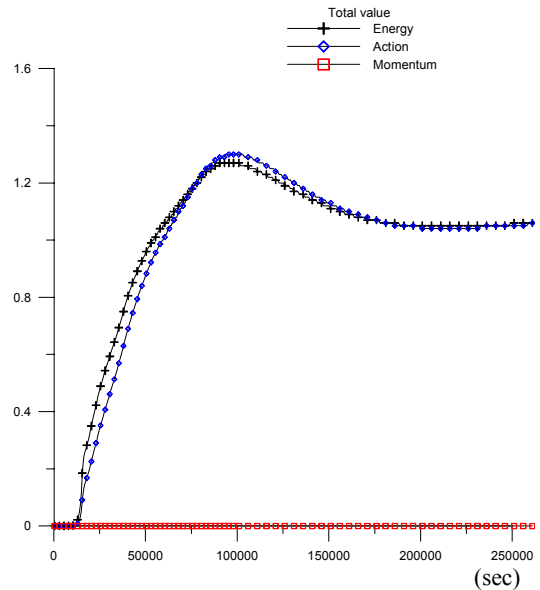


Fig. 3. Evolution of total wave energy, action and momentum in time for isotropic case

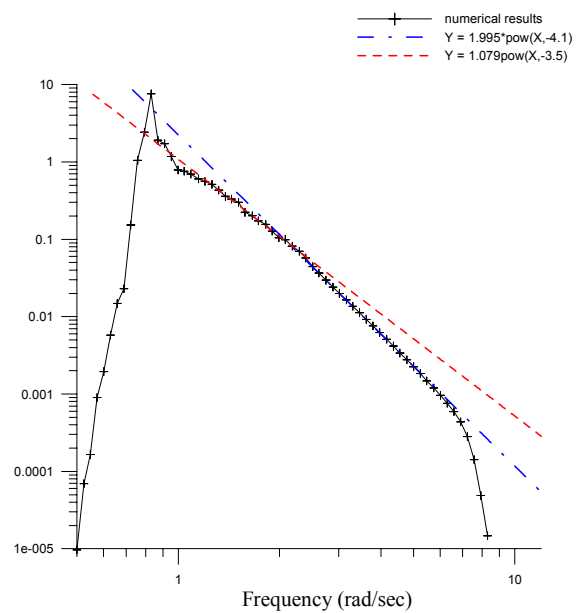


Fig. 4. Stabilised spectrum with two different power dependencies approximated as $S \approx \omega^{-11/3}$ within the range: $1.0 < \omega < 2.0$ and as $S \approx \omega^{-4.0}$ in $2.0 < \omega < 7.0$ (rad/sec)

The frequency first range is estimated as: $2.0 < \omega < 7.0$ (rad/s), where the spectrum can be approximated as $S \approx \omega^{-4.0}$. This frequency domain includes a transparency range $4.0 < \omega < 7.0$ (rad/s), without any energy input or dissipation. The

obtained power approximation $S \approx \omega^{-4.0}$ is based on results of numerical simulations coinciding with analytical solution (Zakharov and Filonenko, 1966).

It should be noted that another part of this range: $2.0 < \omega < 4.0$ (rad/s) with energy input is also approximated by the same dependence: $S \approx \omega^{-4.0}$. This result has not been yet obtained analytically.

In the second frequency range: $1.0 < \omega < 2.0$ (rad/s) the spectrum is approximated with the help of another power dependence $S \approx \omega^{-1/3}$, which is close to analytical solution for inverse cascade of the wave action (Zakharov&Zaslavskii, 1982).

3.2 Balance of source function components

The spectrum form becomes stable for a fully developed stage. It means that a total source function should be equal to zero. However, this balance can be provided differently by various components in appropriate frequency ranges. Source function components for a stabilised case are presented in Fig. 5.

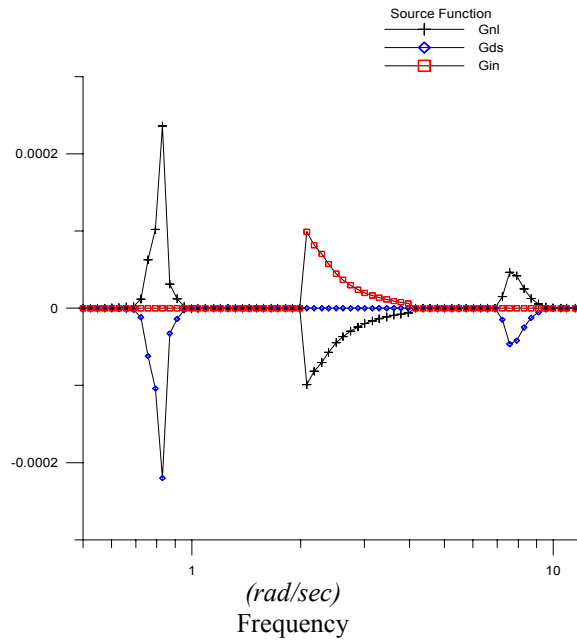


Fig.5. Source function components in different frequency ranges: (+) - non-linear energy transfer, (◇) - wave input, (◁) - dissipation. Positive value of non-linear energy transfer is fully compensated by the dissipation in the low frequency range: $\omega < \omega_1$. At the same time there are no essential value of source function components within the first transparency range $\omega_1 < \omega < \omega_2$.

The wave energy input is balanced by a negative value of non-linear energy transfer within the range of $\omega_2 < \omega < \omega_3$. There is no non-linear energy transfer value within the second transparency range $\omega_3 < \omega < \omega_4$, as it is in case of $\omega_1 < \omega < \omega_2$. Within the high frequency range $\omega_4 < \omega$ the positive value of non-linear energy transfer is balanced by negative value of dissipation.

3.3 Wave energy and action fluxes

It should be interesting to estimate energy and momentum fluxes evolution in wave spectrum. There are different flux components. So, wave energy input flux, coming from the external input source within the range $\omega_2 < \omega < \omega_3$ can be determined as follows:

$$P_{in} = \int_{\omega_2}^{\omega_3} \int_0^{2\pi} f S d\omega d\beta \quad (16a)$$

The wave energy flux directed to low and high frequencies, correspondingly, can be presented similarly:

$$P_{diss}^{low} = - \int_0^{\omega_1} \int_0^{2\pi} \gamma S d\omega d\beta \quad (16b)$$

$$P_{diss}^{high} = - \int_{\omega_4}^{\omega_{max}} \int_0^{2\pi} \gamma S d\omega d\beta \quad (16c)$$

All these values (16a) – (16b) and total value of the wave energy fluxes as a function on time are presented in Fig.6a. As it is seen, the total flux value approaches to zero in time, whereas its various components (16a)-(16c) approach to some non-zero constant values. It can be considered as stabilization of wave evolution process. It should be noted that the value of wave energy flux directed to the high frequency range is approximately 4-fold larger than the same value directed to low frequency range. It means that the external wave energy input flux is mainly expended to high frequency dissipation and only its small part is directed to low frequency wave spectrum development.

The similar values of the wave action fluxes are presented in Fig.6b. It is seen that the wave action flux directed to the low frequency range is significantly larger than its value directed to the high frequency range.

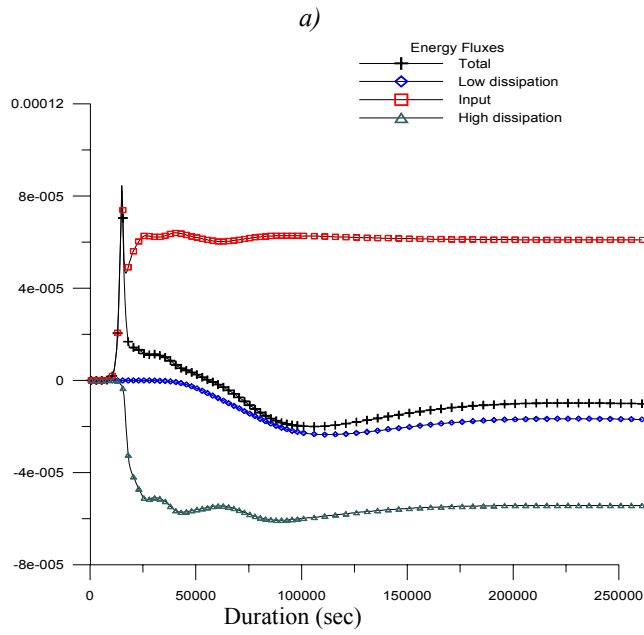


Fig.6 a. Time evolution of wave energy fluxes: total, directed to low frequency range, flux of wave input, and directed to high frequency range

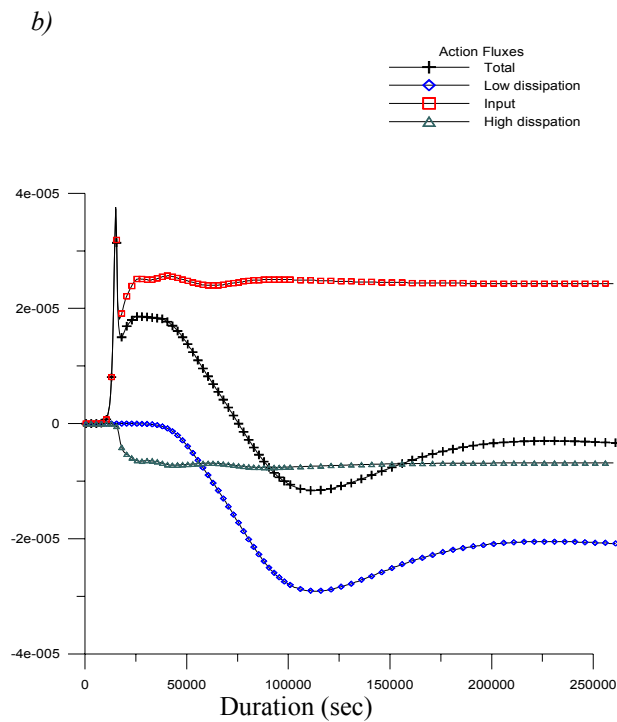


Fig. 6b. Evolution of wave action fluxes directed to different frequency ranges

3.4 Non-isotropic case

Similar numerical simulations are fulfilled for non-isotropic case. External input source function described by cosines angular distribution with power four in (14) is used. Time evolution of total wave energy, action and momentum for non-isotropic case are presented in Fig.7. Frequency spectrum for fully developed stage is presented in Fig.8 and frequency-angular spectrum is in Fig.9.

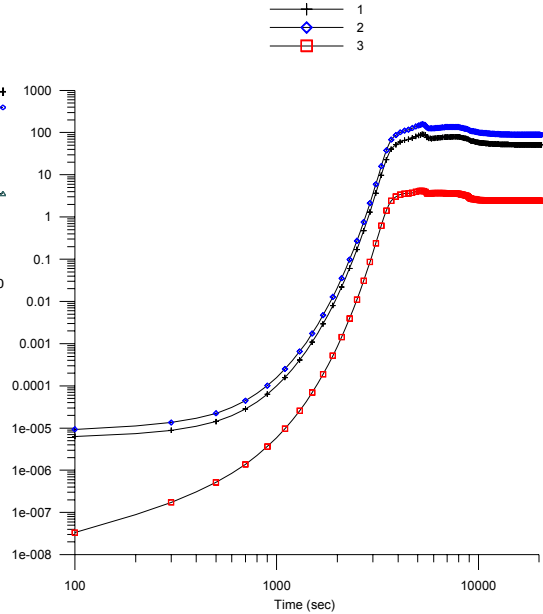


Fig.7. Time evolution for non-isotropic case: 1- total energy, 2- wave action, 3 – momentum

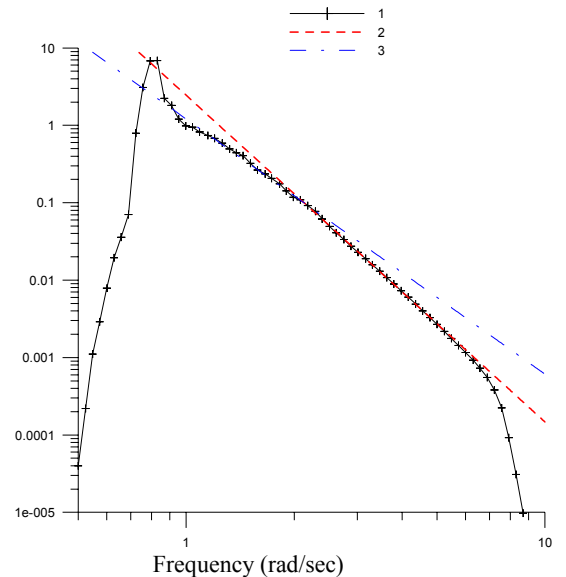


Fig. 8. Fully developed frequency spectrum in non-isotropic case 1 – numerical data , 2- approximation $S \approx \omega^{-4.0}$ 3- approximation $S \approx \omega^{-3.66}$

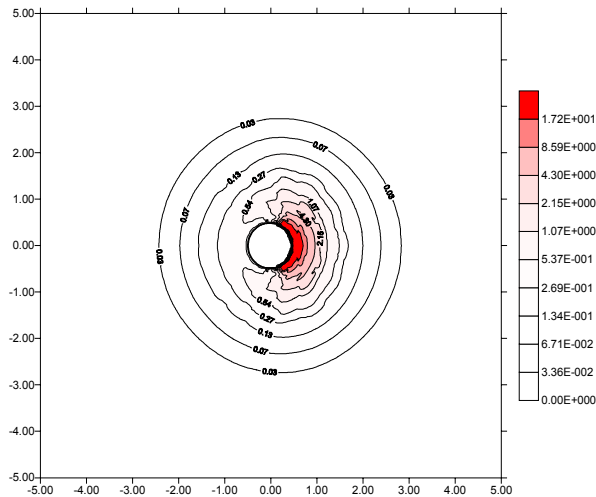


Fig.9. Fully developed frequency-angular spectrum for non-isotropic case

Main results of frequency spectrum numerical simulations reveal approximately the same quantity as in non-isotropic case.

As in the previous case the total energy flux components approach some constant different values. The value of wave energy flux directed to the high frequency range is approximately 4-fold larger than the same value directed to low frequency range. In case of wave action fluxes the opposite situation takes place. Almost the whole value of wave momentum is directed to high frequency range.

3.5 Estimation of relative value of energy, wave action and momentum established fluxes

Relative value of energy, wave action and momentum established fluxes, directed to high and low frequency ranges, correspondingly, should be

estimated. These values for isotropic and non-isotropic cases are presented in Table 1.

According to the results presented in Table 1 the main energy flux is directed to the high frequency range. Its value makes up 77 per cent of total value of wave energy input coming from external source. The main wave action flux is directed to low frequency range. Its relative value is equal to 75 per cent of total wave action of flux input. 25 per cent of wave action is directed to high frequency range. Almost the whole wave momentum (up to 98 per cent) is directed to high frequency range.

4. NUMERICAL SIMULATION WITH MAKIN-KUDRIAVTSEV WIND ENERGY INPUT

Now, numerical simulations with the wind energy input proposed in paper [Makin-Kudriavtsev, 2002] should be carried out. It should be noted that in such a case, the value of the input function becomes negative for waves propagating faster than the wind speed. If dynamical wind pressure on the frontal wave surface is higher in comparison with the rear surface pressure, it causes the appearance of energy flow directed from waves back to atmospheric boundary layer. It is determined by the energy outflux from low-frequency components propagating faster than the wind speed and a relatively small influx to the waves with velocity being close to wind speed.

Numerical simulation is carried out using the above mentioned wind energy input without using low frequency dissipation (13).

The results of numerical simulations for wind speed equal to 20 m/sec are presented in Fig 10 in the logarithmic scale for the following time steps: $t = 3 \cdot 10^4$, 10^5 and 10^6 sec., respectively.

Table 1
Estimation of relative value of energy, wave action and momentum established fluxes, directed to high and low frequency ranges

Input angular distribution	Energy flux to low frequency (%)	Energy flux to high frequency (%)	Wave action flux to low frequency (%)	Wave action flux to high frequency (%)	Momentum flux to low frequency (%)	Momentum flux to high frequency (%)
Isotropic	23.2	76.8	75.3	24.7		
$\cos^2(\beta)$	21.5	78.5	72.7	27.3	1.9	98.1

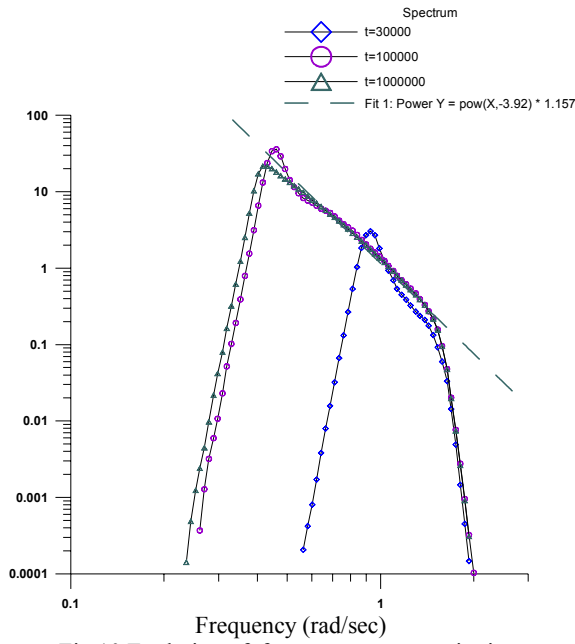


Fig 10. Evolution of frequency spectrum in time

As it is seen the fully established spectrum form is achieved in evolution. It should be noted that fully developed stage is obtained without using a low frequency dissipation (13). Spectrum stabilization is achieved due to low frequency energy flux from wave to atmospheric boundary layer provided by above mentioned mechanism.

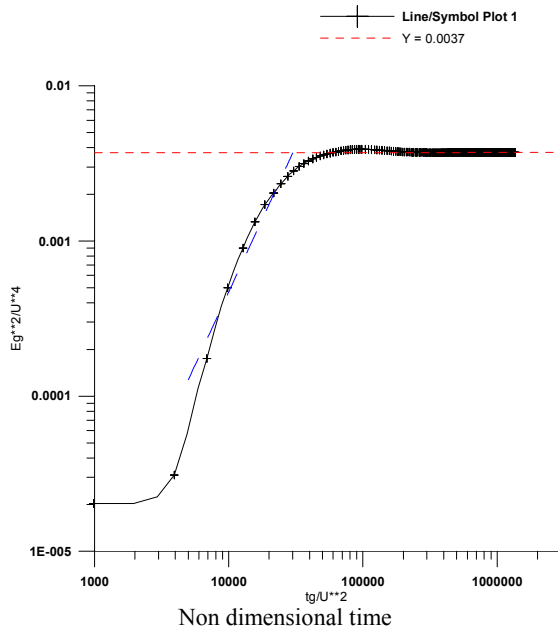


Fig. 11. Evolution of nondimensional wave energy in time with asymptotic

Evolution of nondimensional energy normalized by wind speed value $\tilde{E} = E g^2 / U^4$ is presented in Fig.11. The established value of normalized energy is estimated as $\tilde{E} = E g^2 / U^4 = 0.0037$. It should be pointed out that this value is in good correspondence with the field result analysis equal to 0.0031 (Davidan, 1985).

Source function components for a stabilised case are presented in Fig. 12. A total source function should be equal to zero in stable stage condition achieved at large time. The balance is provided by different components in various frequency ranges. Positive value of non-linear energy transfer function is fully stabilised by dissipation due to backward energy flux in the low frequency range: $\omega < \omega_U$ (where $\omega_U = g / U_{10} \cos(\beta - \beta_U)$). It is produced by wave energy flux going back to atmospheric boundary layer as low frequency waves propagate faster than wind.

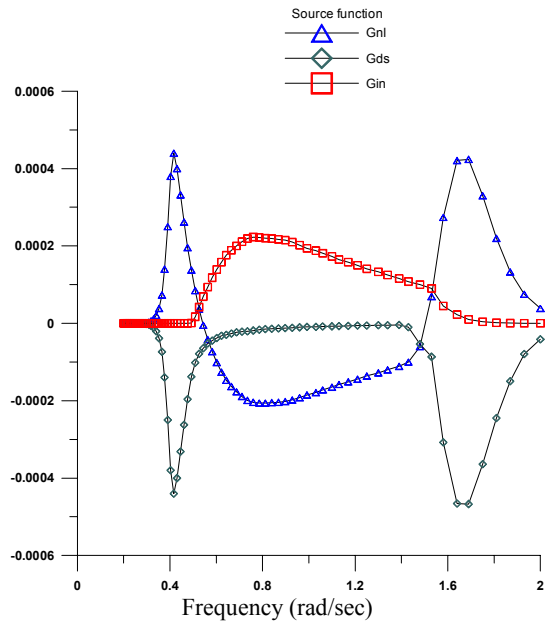


Fig. 12. Source function components : (Δ) - non-linear energy transfer, (\square) - positive wave input, (\diamond) - dissipation

The positive wave energy input coming from wind within the range $\omega_U < \omega < \omega_D$ (where $\omega_D = \omega_4$ - frequency of frequency dissipation range) is balanced by a negative value of non-linear energy transfer within that range.

Within the high frequency range $\omega_D \prec \omega$ the positive value of non-linear energy transfer and wind input is balanced by negative value of dissipation.

The flux evolution of wave energy (Fig.13a), action (Fig.13b) and momentum (13c) to low and high ranges, appropriate wind input and total fluxes are shown in Fig. 13. As it is seen these fluxes approach some constant values in time. At the same time the total energy flux approaches zero.

The same numerical simulations are carried out for wind speed equal to 10 m/sec. The results are similar to the ones obtained previously for 20 m/sec.

Final estimations for relative value of the energy, wave action and momentum stabilized fluxes directed to high and low frequency ranges are presented in Table 2 .

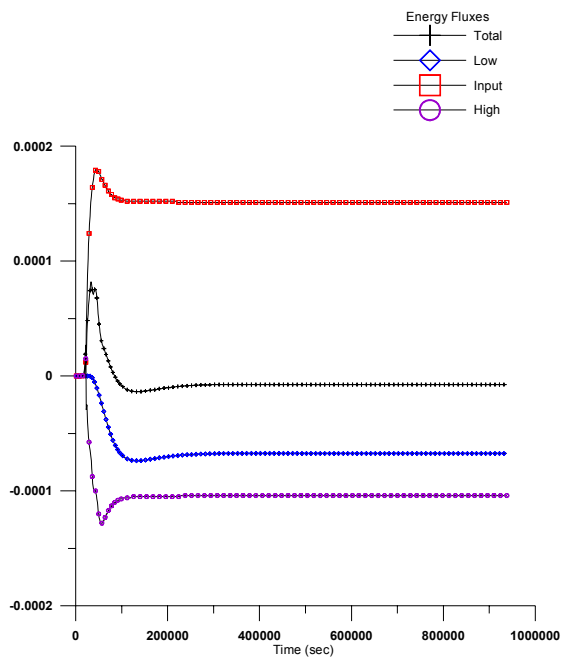


Fig.13 a. Evolution of fluxes wave energy

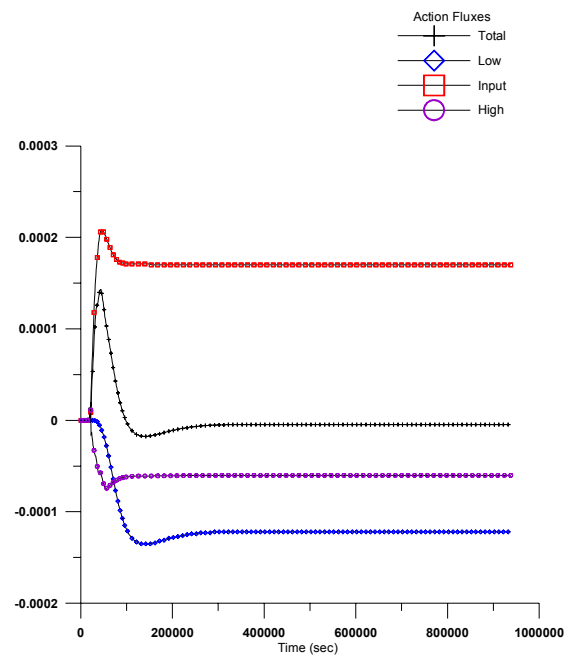


Fig. 13b Evolution of fluxes wave action

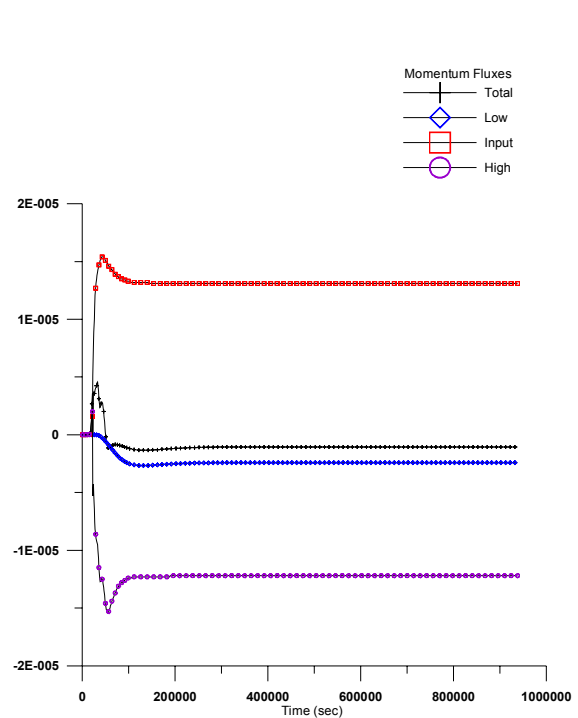


Fig. 13 c Evolution of fluxes wave momentum

It should be noted that similar numerical simulations carried out for spectrum evolution along fetch:

$$C_{gx} \frac{\partial N}{\partial x} = G_{nl} + F - \gamma N \quad (17)$$

provides results very similar to above described for time evolution case.

Table 2

Estimation of relative value of the energy, wave action and momentum stabilized fluxes, directed into high and low frequency ranges

Wind U (m/s)	Energy flux to low frequency (%)	Energy flux to high frequency (%)	Wave action flux to low frequency (%)	Wave action flux to high frequency (%)	Momentum flux to low frequency (%)	Momentum flux to high frequency (%)
20	24.4	75.6	67.0	33.0	3.7	96.3
10	23.4	76.6	66.4	33.6	2.8	97.2

5. NUMERICAL SIMULATIONS USING WAM DISSIPATION

In all the above mentioned numerical simulations the high frequency dissipation function defined by (13) and proposed by V.Zakharov is used. At the same time P.Janssen proposed to produce similar numerical simulations with the help of the WAM model dissipation (4) modified as (Komen et al, 1994):

$$G_{ds} = -C_{ds} \langle \omega \rangle \langle k \rangle^2 m_0^2 \times \left[(1 - \delta) k / \langle k \rangle + \delta (k / \langle k \rangle)^2 \right] N \quad (18)$$

where $C_{ds} = 4.5$ and $\delta = 0.5$, m_0 is a total wave variance, $\langle \omega \rangle$ and $\langle k \rangle$ are the mean angular frequency and mean wave number, respectively.

The dissipation approximation is based on the notion (Hasselmann, 1974) that the wave breaking dissipation can be considered as random distribution of perturbing forces, producing pressure pulsations with small scales in space and time. All the weak processes are supposed to be locally non-linear on the average, simulating a source function, which is quasilinear relatively to interactions of the lowest order. A peculiarity of the dissipation parameterization leads (totally with other items of the source function) to obtain spectra of fully developed sea in the form of the Pierson-Moskovits approximations. The choice of the above dissipation source term (17) over (4) is justified as follows. As it is stated the whitecapping is a process which is weak-in-the-mean, therefore, the corresponding dissipation source term is linear in the wave spectrum. Assuming that there is a large separation between the length scale of the

waves and the whitecaps, the power of the wavenumber in the dissipation term is found to be equal to one. However, for the high-frequency part of the spectrum such a large gap between waves and whitecaps may not exist, allowing the possibility of a different dependence of the dissipation on wavenumbers.

Numerical simulations of the equation (15) are fulfilled using Makin-Kudriavtsev's wind energy input and the above mentioned WAM dissipation. The results for fully developed wind wave spectrum are presented in Fig.14.

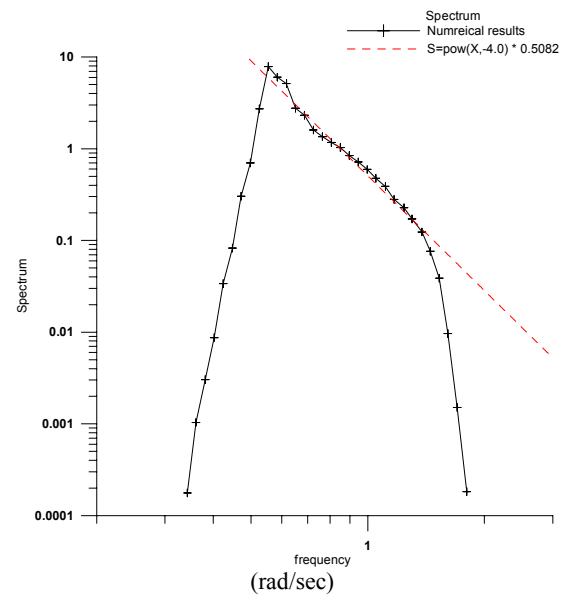


Fig. 14. Fully developed wind wave spectrum with WAM dissipation

Numerical results of source function components with the WAM dissipation are shown in Fig.15. As

it is seen wind wave energy input is fully balanced by non-linear energy transfer and dissipation.

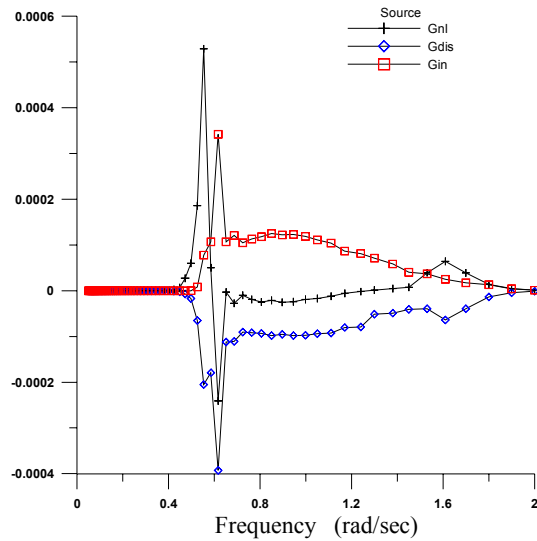


Fig. 15. Source function components with WAM dissipation : (+) - non-linear energy transfer, ([]) - wave input, (\diamond) - dissipation

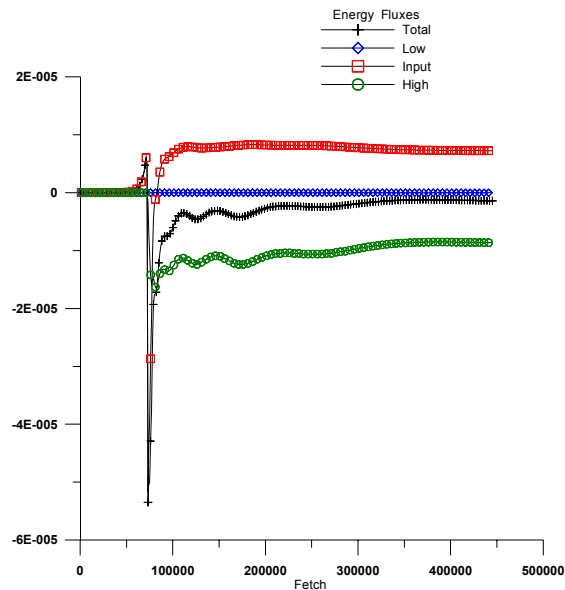


Fig. 16. Wave energy flux evolution

Wave energy flux evolution in time is presented in Fig. 16. There is a balance of source function components for fully developed case. It should be pointed out that the flux of energy directed to low frequency range is completely equal to zero. The same conclusion can be drawn for the fluxes of momentum and action. It means that the WAM dissipation suppresses fully all fluxes directed to low frequency range.

5. DISCUSSIONS

The results of numerical simulations show that there are the main differences between two types of whitecapping dissipation approximations: the WAM dissipation, covering almost the whole frequency range and Zakharov dissipation located in the high frequency range. The values of energy, action and momentum fluxes directed to the high and low frequency ranges differ significantly in these cases.

Numerical simulation of wind wave development with the Makin-Kudriavtsev wind energy input shows that almost 1/4 part of energy flux can be transferred back to atmosphere boundary layer in the low frequency range for a fully developed spectrum. At the same time implementation of the WAM model dissipation reduces almost up to zero all fluxes of energy, momentum and action to low frequency range for fully developed spectrum. There is no energy flux transferred back to atmospheric boundary layer. Thus, a principal difference is shown for physics of wind wave spectrum development and interaction between ocean and atmosphere depending on wave dissipation function.

Until recently it was assumed that the whole energy coming from wind to waves was spent on wave spectrum development and dissipation. However, our results show that it is not quite so. The matter is that the results obtained with the help of Zakharov energy dissipation contrary to WAM dissipation provide the existence of backward energy flux from waves to atmospheric boundary layer. It may reach considerable values (up to 1/4 part of total energy flux) presenting a considerable additional source of energy into atmosphere. The fact should be taken into consideration in global ocean-atmosphere interaction models.

6. CONCLUSIONS

1. Direct numerical simulations of the Hasselmann kinetic equation for gravity waves in water surface are carried out. The spectra are found out to be close to the Zakharov-Filonenko spectrum in the universal (transparency) range. The formation of this asymptotic high frequency spectrum happens explosively.
2. Three different stages can be defined in the wave spectrum evolution. At the first stage the spectrum is quickly increased within input energy range.

High frequency spectrum development is observed at the second stage of spectrum evolution. The frequency spectrum is becoming larger within high frequency range whereas spectral growth is penetrated to a larger frequency range. At the third stage the spectrum evolution is characterized by a slow spectrum development into a low frequency range.

3. Main energy flux is directed to the high frequency range. As for the Zakharov problem formulation high frequency energy flux makes up 77 per cent of the total value of wave energy input coming from external source. The main wave action flux is directed to low frequency range. Its relative value is equal to 67 per cent of total wave action flux input. Some 33 per cent of wave action is directed to high frequency range. Almost the whole wave momentum (up to 98 per cent) is directed to high frequency range.

4. Implementation of the WAM model dissipation reduces almost up to zero all fluxes of energy, momentum and action directed to low frequency range for fully developed spectrum.

5. It is shown that numerical results obtained with the help of Makin-Kudriavtsev wind energy input and Zakharov energy dissipation contrary to WAM energy dissipation provide backward energy flux from waves to atmospheric boundary layer. It may reach essential values (up to 1/4 part of total energy flux from wind to wave) presenting a considerable additional source of energy into atmosphere. Taking into account global process in World ocean this factor should be taken into consideration in weather forecasts and in investigating climate formations.

Acknowledgment. The research presented in this paper was conducted under the grant RFBR 04-05-64306, INTAS-01-234, INTAS-01-2156.

7. REFERENCES

Hasselmann K., 1962. On the non-linear energy transfer in a gravity wave spectrum. Part 1. *J.Fluid Mech.* **12**, 481—500.
Hasselmann, K., 1963. On the non-linear energy transfer in a gravity wave spectrum. Part 2. *J.Fluid Mech.* **15**, 273—281.
Hasselmann S., K. Hasselmann, J.H.Allender and T.P.Barnett, 1985. Computation and parametrisations of the nonlinear energy transfer in a gravity wave spectrum, part 2. Parameterization of the non-linear energy transfer for application in wave models. *J.Physical Oceanography*, **15**,1378-1391.

Komatsu, K., A. Masuda, 1996. A new scheme of nonlinear energy transfer among wind waves: RIAM Method – Algorithm and Performance. *J. of Oceanology.*, **52**,.509—537.

Komen G.J., Hasselmann S., Hasselmann K. 1984. On the existence of a fully developed wind-sea spectrum// *J.Phys.Oceanogr.* Vol.14. —P.1271—1285.

Komen G.J., L.Cavaleri, M.Donelan, K.Hasselmann, S.Hasselmann, and P.A.E.M. Janssen, 1994: Dynamics and Modeling of Ocean Waves. Cambridge: University Press, 532 pp.

Kudriavtsev V.N., Makin V.K. 2004 Impact of swell on the marine atmospheric Boundary Layer. *Journal of Physical Oceanography*, vol. 34, p 934-949

Lavrenov I.V., 2001. Effect of wind wave parameter fluctuation on the non-linear spectrum evolution. *J. Phys. Oceanography*, **31**, N4, 861-873.

Lavrenov I.V. 2003. Wind waves in Ocean. Springer-Verlag, 386pp.

Makin V.K., V.N. Kudriavtsev 2002. Impact of dominate waves on sea drag. *Boundary Layer Meteorology*. 103, 83-99.

Polnikov, V.G., 1993. Numerical formation of flux spectrum of surface gravity waves. *Izv. Acad. Sci. USSR , ser. Physics of Atmosph. and Ocean*, **29**, N6, 1214—1225.

Pushkarev A., D.Resio, V.Zakharov, 2001. Weak turbulent theory of wind-generated gravity sea waves. I Direct Cascade, *Phys. Rev.E* (in print).

Resio, D., W. Perrie, 1991: A numerical study of non-linear energy flux due to wave-wave interaction. Part 1. Methodology and basic results. *J. Fluid Mech.*, **223**, 603—629.

Zakharov, V.E. 1968. Stability of periodic waves of finite amplitude in surface of deep water. *PMFT*, No. 2, 86—94.

Zakharov V.E. 1999. Statistical theory of gravity and capillary waves on the surface of a finite-depth fluid. *Eur.J. Mech. B/Fluids*, 19, 327-344.

Zakharov V.E., N.N.Filonenko, 1966. Energy spectrum of stochastic oscillation in fluid surface *Doklady Acad. Nauk SSSR*, **170**, N6, 1292—1295.

Zakharov V.Ye., M.M. Zaslavskii, 1982: Kinetic equation and Kolmogorov's spectra in in weak turbulent theory of wind waves, *Proc.Acad.Sc.USSR, Atmosphere and Ocean Physics*, Vol.**18**, **9**, 970—980.

Webb D.F., 1978. Non-linear transfer between sea waves. *Deep-Sea Res.* **25**, 279-298.